Çanakkale Onsekiz Mart Üniversitesi Fen Bilimleri Enstitüsü Dergisi, 2019:5,2, 201-213

Çanakkale Onsekiz Mart University Journal of Graduate School of Natural and Applied Sciences, 2019:5,2, 201-213

Araştırma / Research

Fabrication of Nickel Coating on a Stainless Steel Mesh for Supercapacitor Applications

Naime Ozdemir [1]*, Abdulcabbar Yavuz[2], Perihan Yilmaz Erdogan[1], Huseyin Zengin[1]

[1] Gaziantep University, Faculty of Science and Literature Department of Chemistry, Sehitkamil, 27310 Gaziantep, Turkey
[2] Gaziantep University, Engineering Faculty, Department of Metallurgical and Materials Engineering, 27310, Sehitkamil, Gaziantep, Turkey

16.07.2019 Geliş/Received, 29.11.2019 Kabul/Accepted

Abstract

A stainless steel mesh current collector was coated by one-step electrochemical method for supercapacitor applications. As stainless steel mesh has a high surface area, accessibility of ions may be achieved easier than bulk stainless steel. Thin nickel films were synthesized in an aqueous solution electrolyte medium by a three-electrodes electrochemical configuration system under room temperature conditions by applying the potential of -1.5 V for 150, 300 and 600 seconds. The electrochemical capacitive characterization of the prepared nickel films was investigated in 1 M KOH electrolyte solution. The surface morphology of the prepared electrodes was examined. Microstructures of nickel coatings obtained on stainless steel wire surface were similar to tree peels. Therefore, electrodes with high surface area were obtained in the electrodeposition of nickel from pyrophosphate medium. The ion and electron transfer rates between the nickel-coated stainless steel mesh and the alkaline electrolyte were increased. Nickel coated steel mesh having a redox reaction at positive potential between +0.2 V and +0.6 V could be used as cathode electrodes. The nickel/stainless steel mesh electrode has a specific capacity of 1090 F g^{-1} at the scan rate of 5 mV s^{-1}. As the electroactivity of stainless steel in KOH electrolyte was increased with nickel film, nickel-based coatings on stainless steel mesh surface in aqueous solution can be used as cathode electrodes in supercapacitor applications.

Keywords: nickel, stainless steel mesh, electrochemical properties, supercapacitor

Süperkapasitör Uygulamaları için Paslanmaz Çelik Örgü Üzerine Nikel Kaplama Üretimi

Öz

Süperkapasitör uygulamaları için tek adımda paslanmaz çelik örgü akım toplayıcısı elektrokimyasal yöntemle kaplandı. Paslanmaz çelik ağı yüksek yüzey alanına sahip olduğundan, iyonların erişilebilirliği dökme paslanmaz çelikten daha kolaydır. İnce nikel filmler, sulu çözelti elektrolit ortamında, oda sıcaklığı koşulları altında, 150, 300 ve 600

*Sorumlu Yazar (Corresponding Author): Naime Özdemir
(e-posta: naimeozdemir@gmail.com)
Bu makale YÖK 100/2000 Doktora Burs Programı kapsamında yapılmıştır.

saniye boyunca -1.5 V potansiyelinin uygulanmasıyla üç elektrotlu bir elektrokimyasal konfigürasyon sistemi ile sentezlendi. Hazırlanan nikel filmlerin elektrokimyasal kapasitif özellikleri 1 M KOH elektrolit çözeltisinde incelendi. Paslanmaz çelik örgü yüzeyinde elde edilen nikel kaplamaların mikro yapıları ağaç kabuklarına benzemektedir. Bu yüzden, yüksek yüzey alanına sahip elektrotlar, pirofosfat ortamından nikelin elektrodepolanması ile elde edildi. Nikel kaplı paslanmaz çelik örgü ve bazik elektrolit arasındaki iyon ve elektron transfer hızları arttırıldı. +0.2 V ve +0.6 V arasındaki pozitif potansiyelde redoks reaksiyonuna sahip nikel kaplı çelik örgü, katot elektrot olarak kullanılabilir. Nikel/paslanmaz çelik örgü elektrot, 5 mV s^{-1} tarama hızında 1090 F g^{-1} spesifik kapasitansa sahiptir. Paslanmaz çeliğin KOH elektrolitinde elektroaktivitesi nikel filmle karıştırıldığında, sulu çözelti içindeki paslanmaz çelik ağ yüzeyindeki nikel temelli kaplamalar, süperkapasitör uygulamalarında katot elektrodu olarak kullanılabilir.

Anahtar Kelimeler: nikel, paslanmaz çelik örgü, elektrokimyasal özellikler, süperkapasitör

1. Introduction

Recently, many energy storage and conversion devices including capacitors, supercapacitors, fuel cells and batteries have been studied (Arico et al., 2011). Figure 1 displays the specific energy versus specific energies of energy storage devices (Dubal et al., 2013). As the power density of supercapacitor is high, they can be used in energy storage applications. Supercapacitors, called electrochemical capacitors, have been explored by scientists. Supercapacitors have attracted the attention of researchers because of not only their high power density, but also long service life and stability (Jiang et al., 2012). The supercapacitors generally have an electrolyte, a separator (electrically isolates the two electrodes) and two electrodes (Stoller and Ruoff, 2010). The promising applications of supercapacitors include buses, trams and low emission hybrid vehicles (Khaligh and Li, 2010). When used in combination with batteries or fuel cells, supercapacitors with unique properties can function as temporary energy storage devices that provide high power capacity for storing energy without braking.

Supercapacitors are considered into two different categories: electrical double-layer capacitors (EDLCs) and pseudocapacitors. EDLC consist of only electrostatic charge adsorbed in the interface of electrode and electrolyte (Yu et al., 2013). The second type of supercapacitor is pseudocapacitor having faradic reactions between electroactive ions in electrolyte and electrode surface (Conway et al., 1997). Also the combination of these two type capacitors can sometimes considered as the third type of supercapacitor (Carmezim and Santos, 2017). The electrode material constituting the supercapacitor is the most important component of the supercapacitor that characterizes the electrochemical performance (Simon and Gogotsi, 2010). The choice of electrode (anode or cathode) is an important step determining the electrical properties of the supercapacitors (Shi et al., 2014). The most commonly used electrode materials in supercapacitor applications are; carbon based materials (Xian Jian et al., 2016) (in EDLCs), metal oxides/hydroxides (Godillot et al., 2011) and conductive polymers (Wang et al., 2014).

Metal oxides/hydroxides are preferred as electrode materials because of their high specific capacitance and different oxidation states (Kulkarni et al., 2014). Therefore, metal oxides/hydroxides in supercapacitors provide high energy and power generation. Specific capacitance, energy and power measurements are performed by electrochemical cyclic voltammetry (CV) technique. A potentiostat can be used to coat a selected material on the

working electrode surface, and then record the electrochemical performance in an appropriate electrolyte in the range where the redox reaction may occur (Li et al., 2011). In supercapacitor applications, an electrode having a suitable mechanical strength and high capacity should be used. In order to obtain such electrodes, suitable electrode materials and current collectors must be selected (Gamby et al., 2001). Therefore, stainless steel mesh, copper foil and nickel foam can be preferred as a current collector. Stainless steel mesh among them is the most explored surfaces due to their low cost, low toxicity, rough surfaces and easy availability (Vadiyar et al., 2016). They also have excellent mechanical strength for current collectors in energy storage devices (Hu et al., 2009).

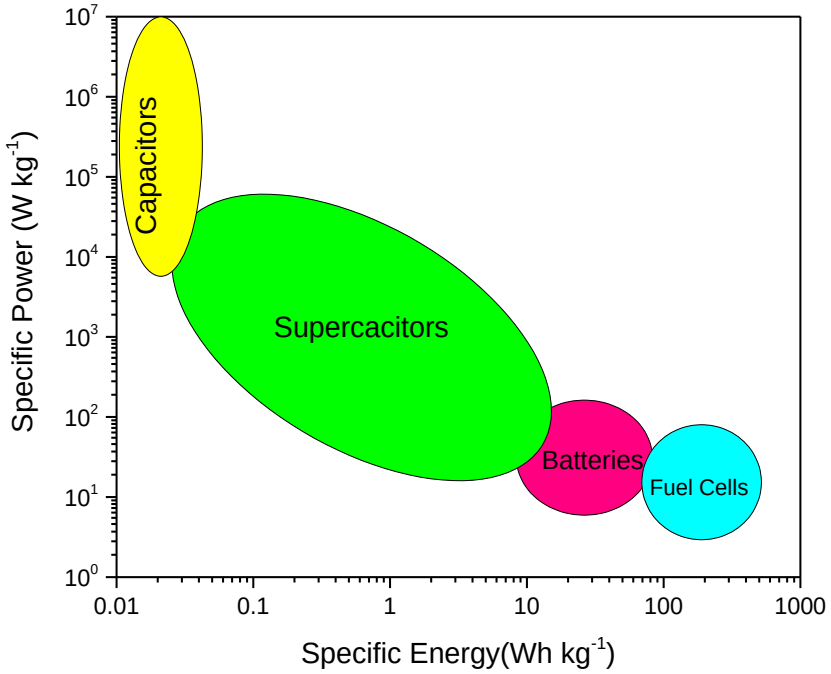

Figure 1: Ragone plot for several energy storage devices (specific power vs. specific energy).

The purpose of this work was to understand the electrodeposition conditions of nickel on a stainless steel electrode by one-step electrochemical method. Nickel-based electrodes were successfully synthesized on a stainless steel mesh without using a binder. After electrodeposition of nickel on stainless steel, it was aimed to examine the microstructures of the coatings. The main aim was to examine electrochemical behavior of a nickel-based coating on a stainless steel mesh in alkaline media. Nickel-based electrodes with three different thicknesses were obtained and specific capacitances with areal capacitances of nickel modified electrodes were calculated. In addition, the electrochemical behaviors of microstructures have been examined by cyclic voltammetry in 1 M KOH electrolyte.

2. Materials and Methods

2.1. Synthesis of Ni-based Electrode

The surface of the stainless steel mesh (Grade 304H) was washed with deionized water prior to electrochemical measurement. The Ni-based electrode was prepared by electrochemical method. The electrodeposition solution was prepared by adding Nickel (II) chloride salt ($NiCl_2.6H_2O$, Merck, 98%) to a solution consisting of 0.7 M potassium pyrophosphate ($K_4P_2O_7$, Sigma Aldrich, 98%) and 0.07 M monopotassium phosphate (KH_2PO_4, Sigma Aldrich, 99%). The electrodes obtained for electrochemical measurements were transferred to

1 M potassium hydroxide (KOH, Merck, 90%) electrolyte. In this study, the chemicals were used directly without any purification process.
The pyrophosphate containing $NiCl_2$ was introduced into the electrochemical cell as deposition electrolyte. Ag / AgCl (sat. KCl) was used as a reference electrode, titanium coated Pt flag was used as a counter electrode and mesh form of stainless steel was used as the working electrode. Stainless steel meshes surface was placed in the pyrophosphate medium containing $NiCl_2$ for electrodeposition. The Ni-based electrode was applied electrochemically to the stainless steel mesh surface by applying -1.5 V for 150sec, 300 sec and 600 sec. All of electrochemical studies took place at room temperature.

2.2. Characterization of the Electrodes

Electrochemical characteristics of the electrodes were examined with a three electrode electrochemical workstation (VersaSTAT 3, AMETEK, Princeton Applied Research, the USA). Electrodeposited Ni on stainless steel mesh electrode was transferred to 1 M KOH electrolyte after they were washed by deionized water. Cyclic voltammetry curves were obtained by scanning at various scan rates from 5 to 100 mV s^{-1}. The surface morphology of the electrodeposited Ni-based film was determined using an upright microscope (Nikon Eclipse LV150NL). Surface morphology was determined with lenses of the magnification of 50X and 100X. The surface morphology of uncoated and coated stainless steel meshes were analyzed in a scanning electron microscope (Gemini 300 SEM, Zeiss) at 1000 and 50 000 magnifications.

3. Results and Discussion

3.1. Electrodeposition of Ni on a Stainless Steel Mesh Electrode

Cyclic polarisation of uncoated stainless steel mesh working electrode scanned from -1.8 V to 0.7 V in the pyrophosphate medium without $NiCl_2$ salt at the scan rate of 50 mV s^{-1} was conducted to determine the potential window of the stainless steel current collector (see red line of Figure 2). Hydrogen evolution reaction started at around -1.0 V on a steel surface (Safizadeh et al., 2015). The deposition voltage of nickel was determined by scanning stainless steel mesh working electrode in pyrophosphate medium in the same voltage range.

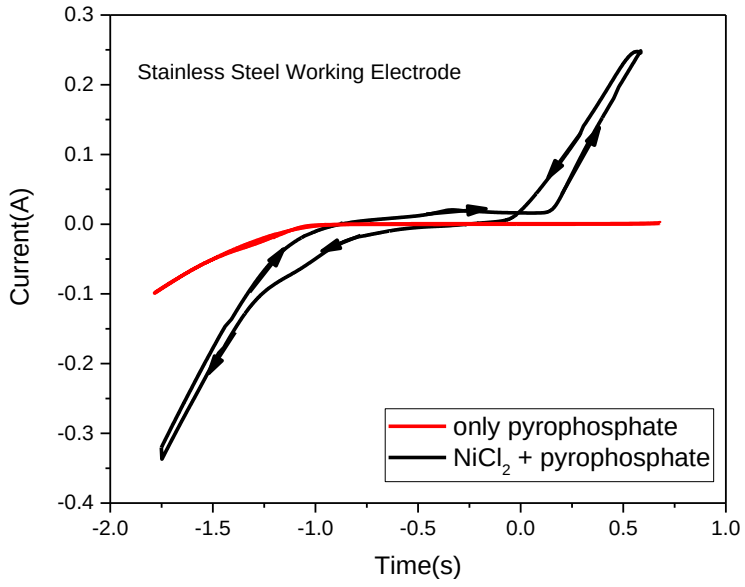

Figure 2: Cyclic polarization curves of uncoated stainless steel mesh current collector in $NiCl_2$-containing (black) and $NiCl_2$-free pyrophosphate medium (red line).

Cyclic voltammetry of stainless steel mesh current collector scanned between the same potentials (from -1.8 V to 0.70 V) in the pyrophosphate medium containing 200 mM $NiCl_2$ was obtained and presented in Figure 2 (black line). A reduction was observed at around -0.75 V when the electrolyte contained Ni^{2+}. As there was no reduction peak without Ni^{2+}, the reduction peak of -0.75 V (black line of Figure 2) belongs to the transformation of Ni^{2+} to nickel metal. Current value of red line (only pyrophosphate electrolyte) was around -0.97 A at -1.8 V. However, the current peak of black line ($NiCl_2$ contained pyrophosphate electrolyte) was around -0.34 V because of the reduction of both Ni^{2+} to Ni and H^+ to H_2. It was determined that the stainless steel mesh electrode could be operated at voltages lower than -1.0 V in pyrophosphate media for electrodeposition of nickel. Nickel electrodeposition can be proved by the oxidation peak of pyrophosphate electrolyte containing $NiCl_2$ started at around 0.2 V. After this potential nickel film was dissolved from the stainless steel mesh surface.

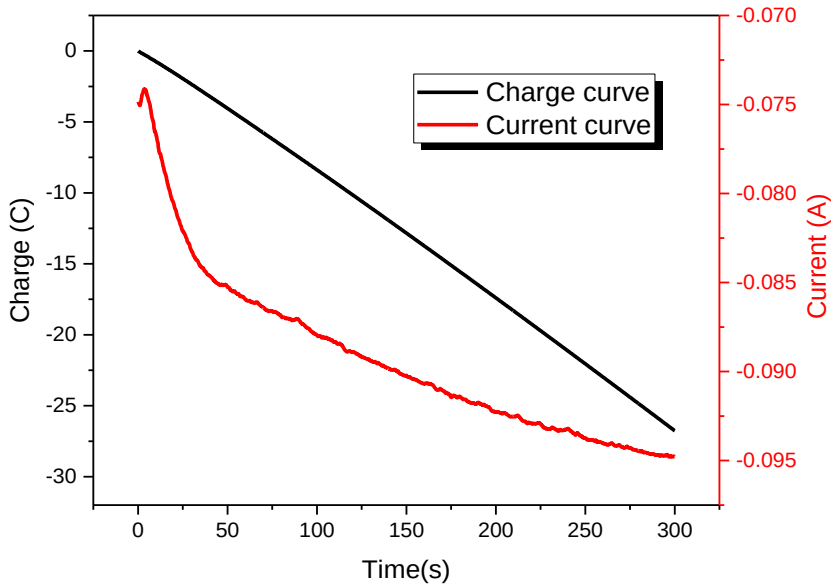

Figure 3: Time vs. current and charge graph of nickel film obtained on stainless steel mesh by applying -1.5 V potential in pyrophosphate medium containing $NiCl_2$.

The applied potential was determined as -1.5 V for electrodeposition voltages of nickel from the pyrophosphate media containing nickel-based salt in this study. Nickel film was obtained by electrochemical method on a stainless steel mesh working electrode by applying -1.5 V for 300 seconds. Figure 3 shows the current and charge versus time graphs for the electrochemical growth of nickel on a steel mesh working electrode by applying a constant potential of -1.5 V. Hydrogen gas was also released as a low voltage was applied during the electrodeposition process. Therefore, the charge value appears to be as high as about 28 Coulombs. This charge occurred not only because of nickel deposition but also hydrogen evolution. Mass of nickel-based films was 262, 119 and 15 µg depending on deposition time of 600, 300 and 150 seconds, respectively.

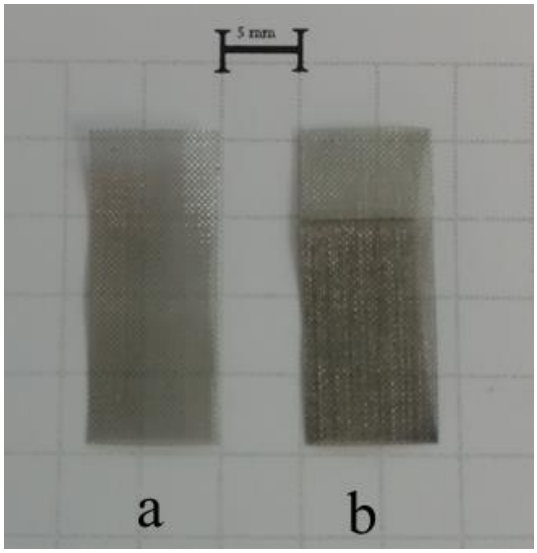

Figure 4: Photographs of (a) uncoated stainless steel mesh surface and (b) nickel film coated by electrochemical method on stainless steel mesh from pyrophosphate containing $NiCl_2$. Each square is 25 mm^2.

3.2. Structural Characterization

The image of the stainless steel mesh current collector before electrodeposition of nickel is presented in Figure 4a. Figure 4b is an image of a nickel-based electrode synthesized electrochemically by applying a potential of -1.5 V for 300 seconds in a pyrophosphate media containing $NiCl_2$. After electrodeposition of nickel on a stainless steel mesh surface, the gray colour of mesh became darker gray as it is seen at the bottom of Figure 4b.

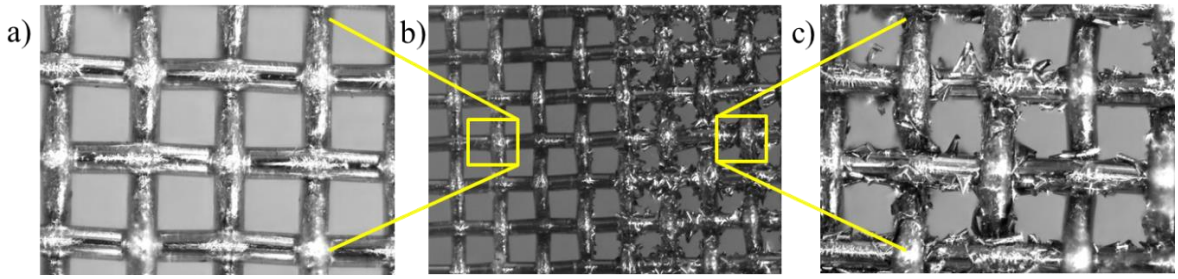

Figure 5: Images of a) uncoated; b) interface of uncoated and nickel coated; c) nickel coated stainless steel mesh surface. Nickel was coated from pyrophosphate electrolyte with $NiCl_2$ salt by applying -1.5 V for 300 seconds. The images were magnified 50X (panel b) and 100X (panel a and c).

Microscope images of the bare and nickel coated mesh electrodes are illustrated in Figure 5. Scanning electron microscopes of uncoated and coated steel mesh are presented in Figure 6. Microscope images of the coating and current collector in two different magnifications (50X and 100X) are presented in Figure 5. Figure 5a shows the steel mesh working electrode has a greater surface coverage than a bulk stainless steel. When the film is electrochemically coated on the stainless steel mesh electrode, it can have a higher surface area than bulk stainless steel surface. Figure 5c illustrates a microscope view of the electrochemically obtained nickel-based film on the stainless steel mesh. Figure 5b illustrates a microscope image of the interface between uncoated and nickel coated mesh current collector. It is observed that the nickel film obtained electrochemically from pyrophosphate media is coated on the surface of the wires not coated in voids of the mesh. This can be observed in SEM images given in

Figure 6c. Figure 5c and in Figure 6c show that the nickel-based coating on the stainless steel surface has a structure similar to tree peels.

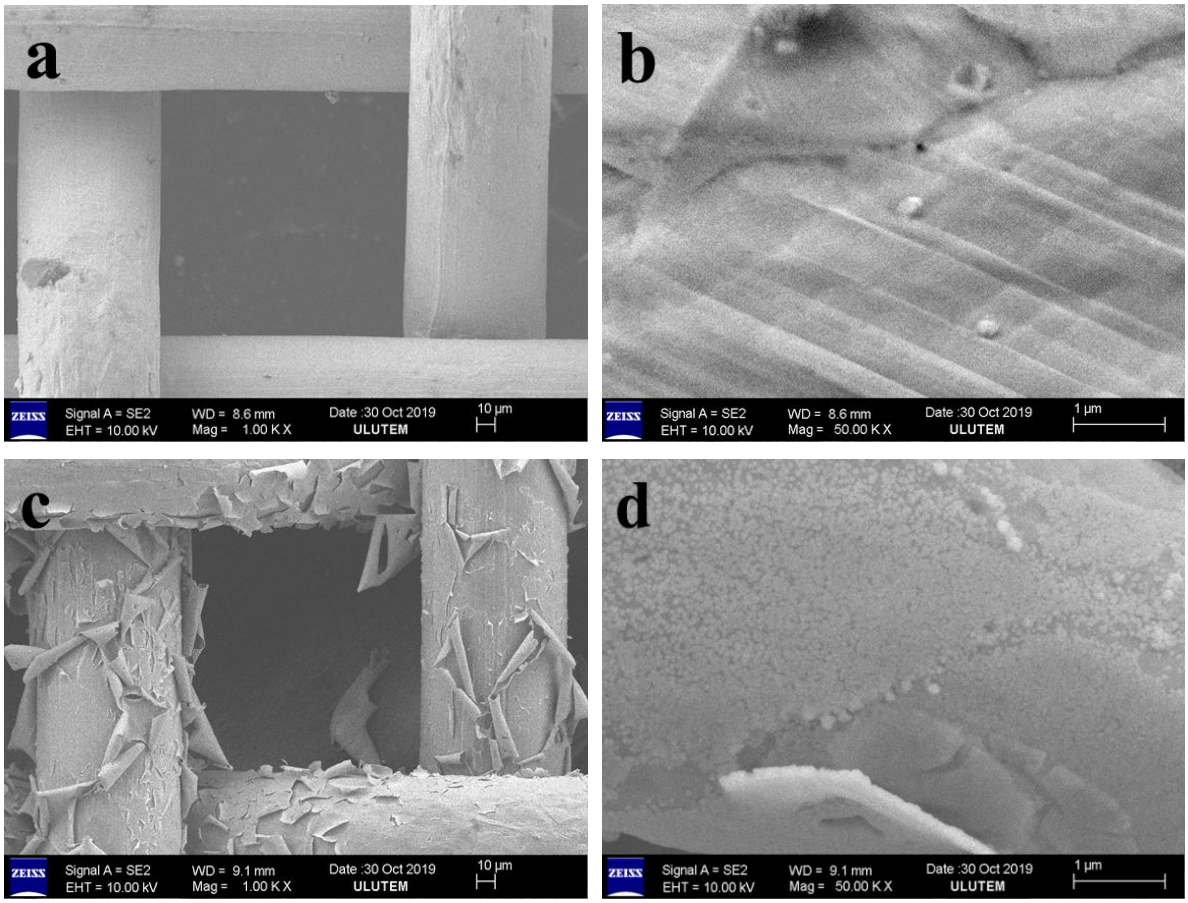

Figure 6: Scanning electrom micrographs of bare stainless steel mesh at a) 1000X magnification, b) 50 000X magnification and Ni coated stainless steel mesh at c) 1000X magnification, d) 50 000X magnification.

3.3. Electrochemical Studies

The nickel-based electrodes were electrochemically obtained on the stainless steel surface. The nickel/mesh electrodes were transferred into 1 M KOH electrolyte to evaluate their electrochemical performances. Figure 7 (red, green and blue lines for different deposition time) represents the cycling voltammogram curve of the nickel-based films in the KOH electrolyte in the potential range from +0.2 V to +0.6 V at 50 mV s^{-1} scan rate. Figure 7 (black line) indicates the voltammetric curves of the bare stainless steel electrode at the scan rate of 50 mV s^{-1} in the KOH electrolyte. The blue, red and green lines of Figure 7 demonstrate that the nickel coated stainless steel mesh had an oxidation/reduction (redox) peak and bare steel (black line of Figure 7) was not electroactive in the KOH electrolyte between +0.2 V and +0.6 V potentials. As nickel coated stainless steel mesh had faradaic reaction in KOH electrolyte and its current collector did not react with alkaline media, this modified electrode could be used as a cathode electrode in energy storage devices.

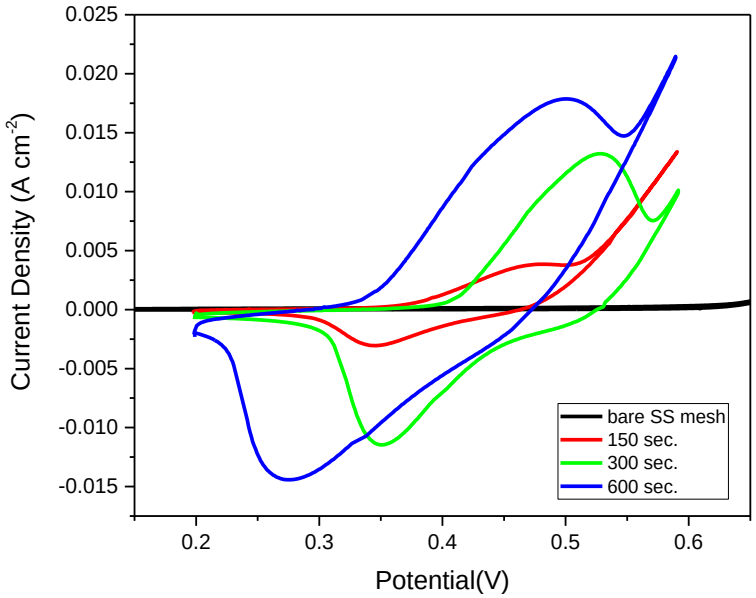

Figure 7: Cycling voltammogram curves of bare stainless steel mesh current collector and nickel coated stainless steel mesh in KOH electrolyte at 50 mV s^{-1} scan rate in the potential window from +0.2 to +0.6 V.

Electrochemical characterization of the nickel/stainless steel mesh electrodes was performed in an alkaline electrolyte. Figure 8 illustrates cyclic voltammogram curves of the coatings obtained on the stainless steel mesh surface in 1 M KOH electrolyte between +0.2 V and +0.6 V cycling at different scan rates (between 5 and 100 mV s^{-1}). During the scans between the oxidation direction (from +0.2 V to +0.6 V) and the reduction direction (from +0.6 V to +0.2 V), a pair of actual peaks corresponding to the reversible transformation was clearly visible. The reaction takes place between reversible displacement reactions of OH^- ions (Wang et al., 2016). When the curves at different scan rates in Figure 8 are examined, the cathodic and anodic peak shifted to more positive and more negative potential values, respectively.

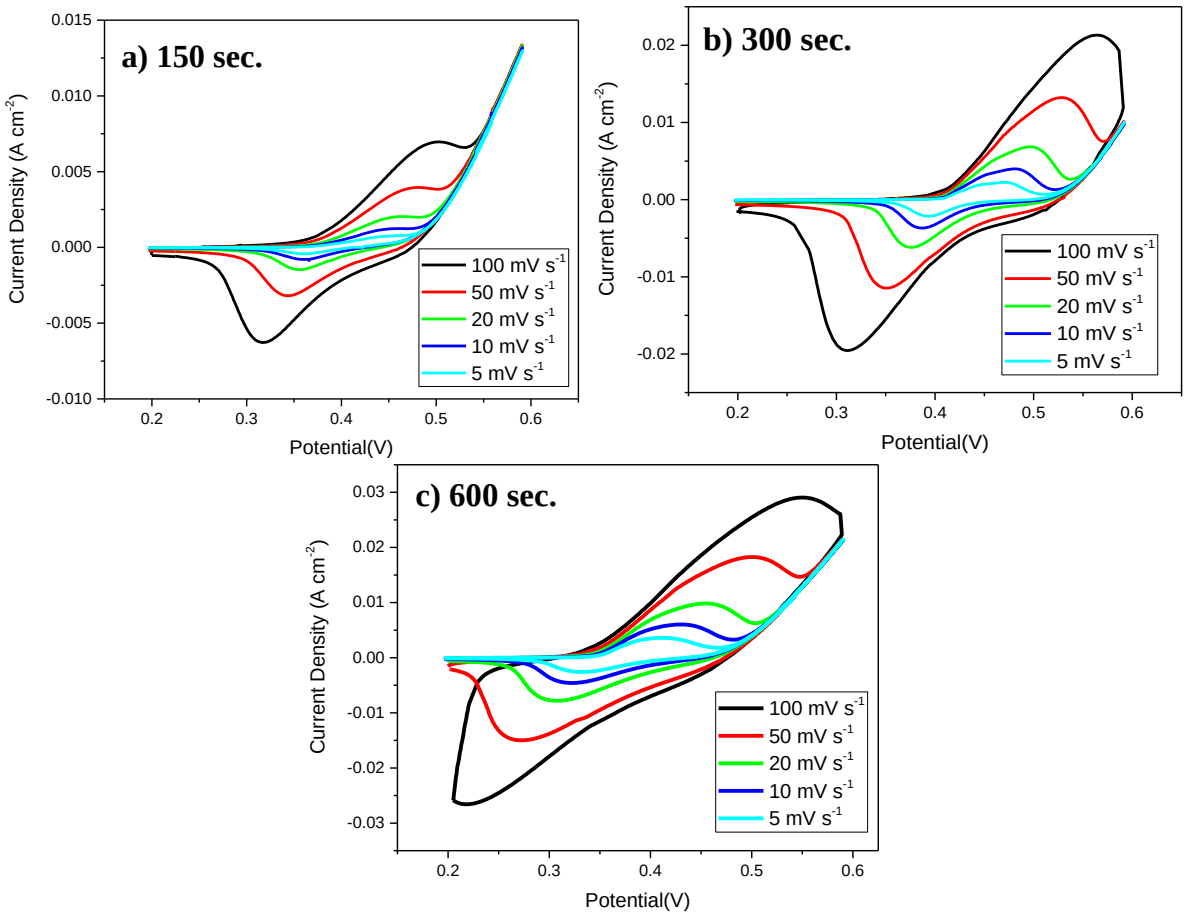

Figure 8: Cycling voltammogram curves of nickel-based electrode in 1 M KOH at various scan rates. Nickel coated electrode was obtained on stainless steel mesh working electrode by applying -1.5 V in pyrophosphate solution containing $NiCl_2$. The electroplating time of nickel growth was a) 150 seconds, b) 300 seconds and c) 600 seconds.

The electrochemical performance of the nickel-based electrode was calculated for their specific capacities at different scan rates. Figure 9 displays the specific capacitance (C_s) of the nickel-based electrodes depending on the scan rates. The magnitude of specific capacitance appears to increase with decreasing the scan rate because of the fact that not all active regions of the electrode were used due to the limited time interval. Specific capacitances of the coatings in F g^{-1} are tabulated in Table 1. The change in capacitance over time is an important factor for supercapacitor applications.

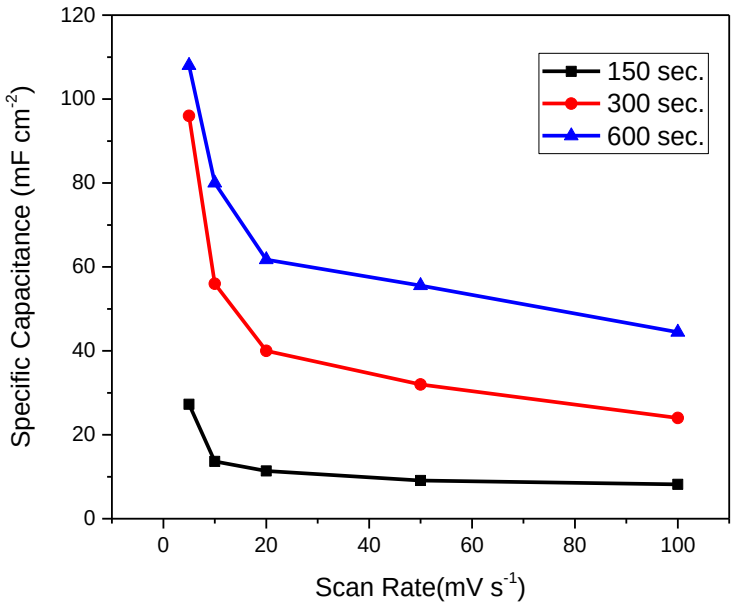

Figure 9 : Specific capacitance of the nickel film on stainless steel mesh in KOH electrolyte for various scan rates. Specific capacitance values shown here were calculated from Figure 8.

The specific capacitance value was calculated based on the voltammetric curves of Figure 8 obtained at the different scan rates from 5 to 100 mV s^{-1}. Areal capacitances increase upon increasing deposition time. However, specific capacitance in F g^{-1} decreases with deposition time because the mass of electroactive film for these films is related to surface area. As the mass of the film obtained at 150 seconds is lower than the mass of other films, the capacitance divided by mass increases. The maximum specific capacitance of the nickel-based electrode obtained on the stainless steel mesh surface was 1090 F g^{-1} at 5 mV s^{-1} scan rate.

Table 1: Specific capacitance of Ni based coating electrodeposited by applying different growth time.

Scan rate (mV s^{-1})	16.8 nm based film (F g^{-1})	133 nm Ni based film (F g^{-1})	293 nm (F g^{-1})
100	545	201	169
50	606	268	212
20	757	335	235
10	909	469	235
5	1090	805	329

4. Conclusions

Ni-based electrode was obtained at room temperature using one-step electrochemical method. Electrodeposition process of nickel was achieved from pyrophosphate medium by applying the potential of -1.5 V for different applied time (150, 300 and 600 seconds) by means of a potentiostat having three electrode cells. Since the rate of electron and ion transportation can be increased in thin films, stainless steel mesh surface could be used as a substrate because its surface area is greater than bulk stainless steel. The stainless steel mesh used as a deposition substrate has a high surface area and the resulting thin film can be coated on a large surface. The obtained nickel-based electrode shows much greater electroactivity in KOH electrolyte than stainless steel mesh used as current collector. Ni-based electrodes could be used as an electrode material in 1 M KOH electrolyte solution for supercapacitor applications. Nickel

coating on stainless steel mesh can be used as cathode electrodes because they have a redox reaction at positive potential range (0.2 V to 0.6 V). The Ni-based films obtained on the stainless steel working electrode had a specific capacity of 1090 F g^{-1} at 5 mV s^{-1} scan rate. High capacitance of nickel coated steel mesh electrodes was obtained for different scan rates. Nickel coated stainless steel mesh surface provided superior redox capacitance and electrochemical performance due to the highly accessible reaction sites of Ni-based films. The electroactivity of stainless steel was normally low in KOH electrolyte. After nickel-based film was coated on steel mesh from an aqueous bath, the capacitance of electrodes was increased significantly. Therefore, these coatings could be used as cathode electrodes in energy storage devices.

Acknowledgements

Authors thank to the YOK-Turkey for the 100/2000 Doctoral Scholarship.

References

Arico A. S., Bruce P., Scrosati B., Tarascon J. M., Van Schalkwijk W., 2011. Nanostructured Materials for Advanced Energy Conversion and Storage Devices. In Materials For Sustainable Energy: A Collection of Peer-Reviewed Research and Review Articles from Nature Publishing Group, World Scientific, 148–59.

Carmezim M. J., Catarina F.S., 2017. Metal Oxides in Supercapacitors Electrolytes in Metal Oxide Supercapacitors. Elsevier.

Conway B. E., Birss V., Wojtowicz, J., 1997. The Role and Utilization of Pseudocapacitance for Energy Storage by Supercapacitors. Journal of Power Sources 66(1–2): 1–14.

Dubal D. P., Gund G. S., Lokhande C. D., Holze R., 2013. CuO Cauliflowers for Supercapacitor Application: Novel Potentiodynamic Deposition. Materials Research Bulletin 48(2): 923–28.

GambyJ., Taberna P. L., Simon P., Fauvarque J. F., Chesneau M., 2001. Studies and Characterisations of Various Activated Carbons Used for Carbon/Carbon Supercapacitors. Journal of Power Sources 101(1): 109–16.

Godillot G., Guerlou-Demourgues L., Taberna P. L., Simon P., Delmas C., 2011. Original Conductive Nano-Co_3O_4 Investigated as Electrode Material for Hybrid Supercapacitors. Electrochemical and Solid-State Letters 14(10): A139.

Hu L., Choi J. W., Yang Y., Jeong S., La Mantia F., Cui L. F., Cui Y., 2009. Highly Conductive Paper for Energy-Storage Devices. Proceedings of the National Academy of Sciences 106(51): 21490–94.

Jiang H., Ma J., Li C., 2012. Mesoporous Carbon Incorporated Metal Oxide Nanomaterials as Supercapacitor Electrodes. Advanced Materials 24(30): 4197–4202.

Khaligh A., Li Z., 2010. Battery, Ultracapacitor, Fuel Cell, and Hybrid Energy Storage Systems for Electric, Hybrid Electric, Fuel Cell, and Plug-in Hybrid Electric Vehicles: State of the Art. IEEE transactions on Vehicular Technology 59(6): 2806–14.

Kulkarni S. B., Patil U. M., Shackery I., Sohn, J. S., Lee, S., Park, B., Jun, S., 2014. High-Performance Supercapacitor Electrode Based on a Polyaniline Nanofibers/3D Graphene Framework as an Efficient Charge Transporter. Journal of Materials Chemistry A 2(14): 4989–98.

Li Z., Wang J., Liu X., Liu S., Ou J., Yang S., 2011. Electrostatic Layer-by-Layer Self-Assembly Multilayer Films Based on Graphene and Manganese Dioxide Sheets as Novel Electrode Materials for Supercapacitors. Journal of Materials Chemistry 21(10): 3397–3403.

Safizadeh F., Ghali E., Houlachi G., 2015. Electrocatalysis Developments for Hydrogen Evolution Reaction in Alkaline Solutions–a Review. International journal of hydrogen energy 40(1): 256–74.

Shi M., Kou S., Yan X., 2014. Engineering the Electrochemical Capacitive Properties of Graphene Sheets in Ionic-Liquid Electrolytes by Correct Selection of Anions. ChemSusChem 7(11): 3053–62.

Simon P., Gogotsi Y., 2010. Materials for Electrochemical Capacitors. In Nanoscience And Technology: A Collection of Reviews from Nature Journals, World Scientific, 320–29.

Stoller M. D., Ruoff R. S., 2010. Best Practice Methods for Determining an Electrode Material's Performance for Ultracapacitors. Energy & Environmental Science 3(9): 1294–1301.

Vadiyar M. M., Bhise S. C., Kolekar S. S., Chang, J. Y., Ghule, K. S., Ghule, A. V., 2016. Low Cost Flexible 3-D Aligned and Cross-Linked Efficient $ZnFe_2O_4$ Nano-Flakes Electrode on Stainless Steel Mesh for Asymmetric Supercapacitors. Journal of Materials Chemistry A 4(9): 3504–12.

Wang K., Wu H., Meng Y., Wei Z., 2014. Conducting Polymer Nanowire Arrays for High Performance Supercapacitors. Small 10(1): 14–31.

Wang R., Xu C., Lee J. M., 2016. High Performance Asymmetric Supercapacitors: New NiOOH Nanosheet/Graphene Hydrogels and Pure Graphene Hydrogels. Nano Energy 19: 210–21.

Jian X., Liu S., Gao Y., Tian W., Jiang Z., Xiao X., Yin L., 2016. Carbon-Based Electrode Materials for Supercapacitor: Progress, Challenges and Prospective Solutions. Journal of Electrical Engineering 4(2): 75–87.

Yu G., Xie X., Pan L., Bao Z., Cui Y., 2013. Hybrid Nanostructured Materials for High-Performance Electrochemical Capacitors. Nano Energy 2(2): 213–34.